Microporous and Mesoporous Materials 154 (2012) 87–92

Contents lists available at SciVerse ScienceDirect

Microporous and Mesoporous Materials

journal homepage: www.elsevier.com/locate/micromeso

Design of activated carbon–clay composites for effluent decontamination

M. Yates [a,*], M.A. Martín-Luengo [b], L. Vega Argomaniz [a], S. Nogales Velasco [a]

[a] Institute of Catalysis and Petroleochemistry (CSIC), Calle Marie Curie 2, Cantoblanco, 28049 Madrid, Spain
[b] Institute of Materials Science of Madrid (CSIC), Calle Sor Juana Ines de la Cruz 3, Cantoblanco, 28049 Madrid, Spain

ARTICLE INFO

Article history:
Received 26 May 2011
Received in revised form 8 July 2011
Accepted 12 July 2011
Available online 16 August 2011

Keywords:
Activated carbon
Gas purification
Ceramic composites
VOCs

ABSTRACT

Adsorption offers an efficient technology for removing volatile organic compounds (VOCs) from air pollution sources. Often activated carbons (ACs) are employed owing to their large specific surface areas, high micropore volumes, rapid adsorption capabilities and selectivity towards organic molecules compared to water vapour or air. However, when large volumes of gas are to be treated pressure drop limitations may arise from the use of conventional powder adsorption beds. For these applications conformation of the activated carbon as open channel honeycomb monoliths can take advantage of the almost null pressure drop caused by these structures. Similarly, conformation as extrudates or tubes although increasing the pressure drop due to the turbulent gas flow can improve any diffusion limitations that the open channel monoliths can suffer. Conformation of the AC as a ceramic composite also improves the handling characteristics. By the use of a silicate clay binder a commercially available AC, was conformed in three different monolithic geometries; changing the channel width and the wall thicknesses and as solid extrudates and tubes. The textural and mechanical properties of these conformed composite structures were determined and the results analysed along with their dynamic adsorption capacities towards toluene at 30 °C, used as a probe molecule to establish criteria by which the most suitable structure for industrial use could be selected.

1. Introduction

In relation to price/performance, physical adsorption is the most important technique to control air pollution. It is well known that the efficiency of ACs as adsorbents is due to their high micropore volumes and large specific surface areas [1–3]. The adsorption capability of these materials is further enhanced due to their selectivity towards organic vapours compared to water vapour or air [4–6]. In systems that require the treatment of large volumes of gas conventional adsorption beds can suffer from limitations due to the pressure drop. For these applications conformation of the adsorption bed as an array of honeycomb monoliths take advantage of the almost null pressure drop to which these open channel structures give rise [7]. However, these structures may suffer from diffusion limitations both of the gas travelling through the channels before striking the walls, leading to a minimum length requirement and also of the gas to be treated into the porous walls of the structure to the micropores of the material where the contaminants can be trapped. Thus, to study these phenomena a series of AC/clay ceramic composites were prepared in monolithic forms with different wall thicknesses and channel widths and as solid and tubular extrudates. The adsorption capacities of all these structures towards toluene at 30 °C, chosen as a probe molecule, were determined.

Results obtained previously by the authors [8,9] have shown that the static adsorption capacities of several commercially available ACs, conformed as ceramic composites, were related to both the vapour pressure of the gas to be adsorbed and the pore size distribution of the composites. Thus, for toluene adsorption at room temperature, for all the composite materials tested, the static adsorption capacity was found to be equivalent to the pore volume of the material in pores below approximately 140 nm. However, the dynamic adsorption capacity determined by measuring the breakthrough curves of a spiked air flow passing through the adsorption bed was at best found to be directly related to the micropore volume of the composite. However, this optimum value was only attained if the contact time between the air stream to be treated and the open channel monolithic adsorption bed was at least one second, the external surface area of the composite, determined from a *t*-plot analysis was sufficiently large, close to 100 $m^2 g^{-1}$ and the threshold diameter determined by mercury intrusion porosimetry was wider than at least a micron to avoid diffusion limitations [10]. Under these conditions the adsorption bed offers a sufficiently large easily accessible external surface area where the initial adsorption of the organic takes place that allows time for the slower diffusion into the narrow micropores where the contaminant is more strongly adsorbed.

* Corresponding author. Tel.: +34 91 585 4941; fax: +34 91 585 4760.
E-mail addresses: myates@icp.csic.es (M. Yates), mluengo@icmm.csic.es (M.A. Martín-Luengo).

1387-1811/$ - see front matter © 2011 Elsevier Inc. All rights reserved.
doi:10.1016/j.micromeso.2011.07.006

The mechanical strength of the monoliths heat-treated at 150, 500 and 850 °C was also determined and related to the measured porosities of the composite materials in order to try and obtain criteria by which a general porosity/strength relationship could be determined.

2. Experimental

2.1. Composite preparation

In this study Fluesorb B (Chemviron Carbon) was chosen as the AC while α-sepiolite a magnesium silicate clay (Pansil 100 supplied by Tolsa S.A.) was used as the agglomerating agent to achieve the correct rheological characteristics when mixed with the AC and water for the conformation of the materials in monolithic, solid or tubular shapes. Four compositions were prepared with 100, 75, 50 or 25 wt.% of clay binder and the remainder being AC. After premixing of the dry powders by careful addition of water a dough was formed that was fed to a Bonnot single screw extruder and subsequently extruded as honeycomb monolithic structures with parallel channels of square section with channel widths of 2.6, 2.0 and 2.0 mm and wall thicknesses of 0.9, 1.1 and 0.6 mm to give cell densities of 8.1, 10.7 and 14.9 respectively, or as solid extrudates with a 3 mm diameter or as tubes with an external diameter of 3 mm and an internal diameter of 1.7 mm. These materials were first dried at room temperature for three days then heat-treated at 150 °C in air or at 500 or 850 °C in nitrogen at a heating rate of 5 °C min^{-1} to the final temperature which was maintained for 4 h and the material then allowed to cool back down to ambient. Heat-treatment in an inert atmosphere was necessary to avoid combustion of the AC which otherwise begins to occur at about 300 °C. These materials were subsequently used in all of the characterisation techniques and adsorption performance tests.

2.2. Characterisation techniques and adsorption tests

Nitrogen adsorption/desorption isotherms at −196 °C were determined using a Thermo Electron Corporation Sorptomatic 1990. Samples previously heat-treated at 150 °C were outgassed overnight at this temperature; other samples were outgassed at 300 °C to a vacuum of $\leqslant 10^{-2}$ Pa to ensure a dry clean surface free from any loosely held adsorbed species. The specific surface areas (S_{BET}) were calculated by application of the BET equation [11] taking the area of the nitrogen molecule as 0.162 nm^2 [12]. For the raw clay material heat-treated at 850 °C the linear range of the BET equation was located between 0.05–0.35 p/p°, however, for all other materials studied due to their microporous natures this linear range was much narrower and displaced to lower relative pressures: p/p° = 0.02–0.10. The micropore volume and external surface area, i.e. the area not associated with the micropores, were calculated using a *t*-plot analysis [13], taking the thickness of an adsorbed layer of nitrogen as 0.354 nm and assuming that the arrangement of nitrogen molecules in the film was hexagonal close packed [14]. The mesopore volumes of the materials were calculated from the volume of gas adsorbed at a relative pressure of 0.96 on the desorption branch of the isotherms, equivalent to the filling of all pores below 50 nm, minus any microporosity calculated from the corresponding *t*-plot.

Mercury intrusion porosimetry (MIP) analyses were employed to determine the pore size distribution (PSD) and pore volume over the range of 300 μm down to 7.5 nm diameter, utilising CE Instruments Pascal 140/240 apparatus. The pressure/volume data were analysed by use of the Washburn Equation [15] assuming a cylindrical nonintersecting pore model, taking the mercury contact angle as 141° and surface tension as 484 mN m^{-1} [12]. For this technique the samples were previously dried at 150 °C overnight. The total pore volumes and pore size distributions of the conformed materials were determined by combination of the results obtained from nitrogen adsorption/desorption with those obtained from MIP.

The mechanical strengths of the conformed materials were determined using a Chatillon LTCM Universal Tensile Compression and Spring Tester with a test head of 0.79 mm diameter. For these tests the results obtained with the monolith with a 2.6 mm channel width were determined. The test head was positioned over one of the channel walls of the corresponding monolith and the pressure slowly increased until rupture of the wall was caused. The average of ten measurements for each sample was taken to ensure the accuracy and precision of the results.

Dynamic adsorption measurements on the monolithic samples were carried out in a glass reactor with an internal diameter of 2.54 cm at 94 kPa and a bed temperature of 30 °C. The monolithic samples, of nine channels 3 × 3 and 14 cm in length, were first dried overnight at 150 °C and then weighed. The monolith was then loaded into the reactor and the space between the external walls of the monolith and the internal wall of the reactor filled with silicon carbide with an average particle diameter of 0.84 mm to ensure that the gas flowed through the monolith channels. The samples were then preconditioned at 150 °C in a dry air stream overnight, cooled to 30 °C and the air stream switched to one containing 100 ppm of toluene. The gas flows were adjusted for each monolithic sample to maintain a constant contact time of 0.25 s. For the solid extrudates and the hollow tubes the samples were cut to 0.5 mm lengths and the same volume of material was used as that occupied by the wide channel monolith. In this way the same contact time was achieved since the bed volume was maintained constant. For experiments with these materials a reactor with a 1 cm internal diameter was employed in order to achieve a similar bed depth to that used with the monolithic samples. The toluene concentration was controlled by bubbling air through the organic maintained in a thermostatic bath at approximately −11 °C and then diluting this spiked stream with further air. The concentrations at the inlet and outlet were measured with a sensitivity of ±0.1 ppm by means of a Horiba THC FID (model FIA-510) and the breakthrough point was taken when 10 ppm of toluene was detected in the exit gas.

3. Results and discussion

3.1. Textural properties of the raw materials

Since in the fabrication of the commercial AC employed in this study temperatures in excess of 850 °C were used, the textural data acquired with this sample was considered to be unchanged with the heat-treatment of the composite materials. The AC had a primary particle size of 90% <12.3 μm, a specific surface area (S_{BET}) of 912 $m^2 g^{-1}$ of which 55 $m^2 g^{-1}$ were due to the external area, with a micropore volume of 0.38 $cm^3 g^{-1}$ and a mesopore volume of 0.10 $cm^3 g^{-1}$. For the clay used in this study, with a much smaller particle size of only about 0.3 μm, heat-treatment at the three temperatures used caused a decrease in the measured surface areas and microporosities of the material due to loss of constitutional water above 350 °C and a phase change to enstatite above 827 °C. After drying at 150 °C the clay had a specific surface area (S_{BET}) of 249 $m^2 g^{-1}$ of which 126 $m^2 g^{-1}$ were due to the external area and micro and mesopore volumes of 0.05 and 0.35 $cm^3 g^{-1}$, respectively. With heat-treatment at 500 and 850 °C the surface areas fell to 138 and 61 $m^2 g^{-1}$ and the external areas to 116 and 50 $m^2 g^{-1}$ with meso and micropores of 0.42, 0.42 and 0.01 and 0.01, respectively. The S_{BET} in the case of microporous materials

Table 1
Textural characterisation of the conformed materials and the AC.

Sample	Heat treatment (°C)	Surface area S(BET) ($m^2\ g^{-1}$)	External area ($m^2\ g^{-1}$)	Micropore volume ($cm^3\ g^{-1}$)	Mesopore volume ($cm^3\ g^{-1}$)	Macropore volume ($cm^3\ g^{-1}$)	Total pore volume ($cm^3\ g^{-1}$)	Mechanical strength (MPa)	Dimensional stability (%)
Pansil 100/AC	150	249	126	0.05	0.39	0.06	0.50	2.86	85.11
100/0	500	138	116	0.01	0.42	0.11	0.54	2.62	84.49
	850	61	50	0.01	0.42	0.12	0.54	4.21	81.97
Pansil 100/AC	150	403	118	0.12	0.32	0.17	0.61	3.17	89.20
75/25	500	350	112	0.10	0.33	0.23	0.66	1.26	88.00
	850	289	62	0.10	0.26	0.24	0.59	3.71	86.50
Pansil 100/AC	150	530	95	0.19	0.26	0.31	0.75	1.36	92.00
50/50	500	529	96	0.19	0.27	0.37	0.82	1.13	91.40
	850	508	57	0.20	0.23	0.39	0.81	2.69	90.20
Pansil 100/AC	150	766	69	0.31	0.21	0.39	0.90	0.74	98.00
25/75	500	731	83	0.28	0.22	0.43	0.93	0.26	97.00
	850	701	82	0.27	0.20	0.44	0.91	1.68	95.50
Fluesorb B		912	55	0.38	0.10				

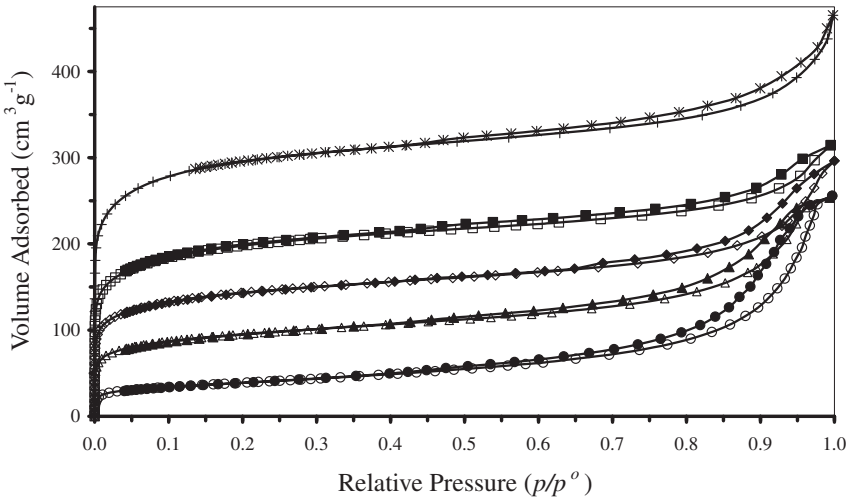

Fig. 1. Nitrogen adsorption isotherms for conformed materials heat-treated at 500 °C Pansil 100/AC: 100/0 ○●, 75/25 △▲, 50/50 ◇♦, 25/75 □■ and Fluesorb B +⁎.

should be considered as an apparent surface area due to the associated micropore filling mechanism [16]. The external area and micropore volumes were calculated from analysis of the *t*-plot of the corresponding isotherms. The pore volume in pores below 50 nm was determined from the amount of gas adsorbed at a relative pressure of 0.96 on the desorption branch of the isotherm, equivalent to the filling of all pores below 50 nm, the mesopore volumes were calculated from the difference between this value and the micropore volume previously calculated from the corresponding *t*-plot.

From the textural characterisation data collated in Table 1 for the four conformed materials it may be observed that the surface area, micro and mesopore volumes of the composites were close to those expected for purely physical mixtures of the two raw materials heat treated at 150, 500 or 850 °C, indicating that there was no significant chemical interaction between the two components during fabrication and subsequent heat-treatment. The dimensional stability of the materials in the final column of Table 1 refers to the shrinkage of the conformed materials. This shrinkage is mainly due to the loss of water originally added to produce a paste with adequate rheological properties for the extrusion of the materials. With all of the conformed materials approximately 50 wt.% of the extruded body is due to the water added in order to successfully extrude the pastes. With drying at 150 °C most of this water is lost causing the dramatic shrinkage of the structure. Heat-treatment at 500 and 850 °C caused further slight reductions in the dimensions of the conformed bodies. It should also be noted that as the percentage of AC was increased the changes in the dimensions of the conformed bodies compared to those of the die used during their extrusion were reduced. This is to be expected since the AC does not undergo any chemical or physical changes with drying and heat-treatment in an inert atmosphere, unlike the clay agglomerating agent.

The nitrogen isotherms for the AC raw material and the conformed materials after heat-treatment at 500 °C are presented in Fig. 1. The microporous nature of the AC is evident from the type I isotherm. The isotherm obtained with the conformed clay is of type IIb [16] with a H3 hysteresis loop, typical of clay materials with a wide poorly defined mesopore size distribution that extends into the macropore range. The isotherms obtained with the composite materials fell between these two extremes, being of mixed type I/II since they displayed characteristics of the two raw materials used in their production.

From the data presented in Table 1 it may be observed that the mechanical strengths of the materials on drying at 150 °C were higher than those obtained after heat-treatment at 500 °C, necessary to form the stable ceramic bodies. This fall in mechanical strength was due to the increase in the meso and macroporosity caused by the losses in the various types of water associated with the clay binder. However, after treatment at 850 °C all materials displayed a

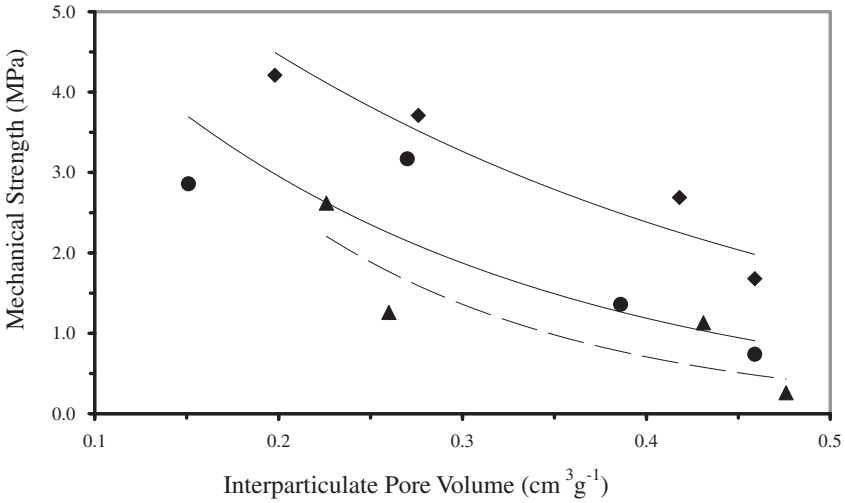

Fig. 2. Relationship between the mechanical strength and the interparticulate porosity for conformed materials heat-treated at 150 °C ○●, 500 °C △▲ and 850 °C ◇♦.

marked improvement in their strengths due to the phase change in the clay. It should also be observed that as the content in the AC was increased the mechanical strength decreased. The decrease in the mechanical strength with increasing AC content was due to two factors, the first being the reduction in the percentage of clay agglomerating agent which binds the structure together and the second the increase in the total pore volume but especially in the width of the widest macropores due to the large particle size of the AC employed. Although using an AC with a smaller primary particle size leads to an increase in the mechanical strength for composites with the same amount of clay binder [8,9]. The relationship between the mechanical strength and the interparticulate porosities of the conformed materials heat-treated at all three temperatures are presented in Fig. 2. From this figure it may be appreciated how for each series the strength development depends on both the amount of AC incorporated and the heat-treatment [9,17].

The total pore volumes and the pore size distributions of the conformed materials heat-treated at 500 °C are shown in Fig. 3. The first inflection in the curves at the widest pore diameters is usually termed as the threshold diameter and can be considered as the limiting diameter for any transport processes into the interior of the porous structure. The position of this inflection is related to the primary particle size of the AC and is of great importance during dynamic adsorption since it may cause mass transfer limitations that reduce the efficiency of the adsorption unit [10]. Thus, although a wide threshold diameter was a requirement for high dynamic adsorption efficiencies to avoid diffusion limitations, a practical limit is met due to the requirement for an adequate mechanical strength and the ease of conformation of the ceramic composite by extrusion, especially in materials with a high percentage of AC and narrow walls.

3.2. Dynamic adsorption capacities

It had been previously demonstrated that the dynamic adsorption capacities for monolithic adsorption units based on ACs were, at best, equivalent to their micropore volumes [10]. However, in order to achieve this optimum behaviour, external surface areas of more than *c.* 100 $m^2\ g^{-1}$ and threshold diameters of greater than 1 μm were necessary with a contact time of at least one second. In this study in order to determine the importance of the conformed shape of the adsorption bed the contact times were reduced to just 0.25 s and the breakthrough point with a 100 ppm toluene stream was taken at 10 ppm. For the wide channel monoliths heat-treated at 500 °C developed in this study the breakthrough curves for the four different compositions are shown in Fig. 4.

From this figure it may first be noted that the dynamic adsorption capacity of the clay used as the agglomerating agent was almost negligible. The breakthrough times were 0.3, 6.0, 6.5 and 12.0 h respectively, for the samples with 0, 25, 50 and 75 wt.% AC. It is interesting to note how the breakthrough time was greatly increased with the incorporation of 25 wt.% AC compared to the clay monolith but these times were not extended by similar amounts with further increases in AC content to 50 and 75 wt.%. This along with the recorded shape of these breakthrough curves points to the diffusion limitation effects that were caused by working at very low contact times.

Taking the samples that had been prepared with a 50:50 wt.% ratio of clay and AC a further set of adsorption experiments were carried out with all the conformations at the same 0.25 s contact time. From the results shown in Fig. 5 the differences caused by the change in the geometries was obvious. For the monolith samples the wide channel material had a breakthrough point after 6.5 h, reduction of the channel width to 2 mm but maintaining the wall thickness of 1 mm increased the breakthrough time to 31.9 h whereas the narrow channel/narrow wall monolith reached its breakthrough after only 20.2 h. However, it must be remembered that all of these experiments were carried out with 14 cm long nine channel (3 × 3) monoliths and thus the weight of material in the adsorption bed was different. Thus, when these breakthrough times are converted into the amount adsorbed against the normalised volume of the adsorption bed the results were 0.030, 0.129 and 0.131 $ml_{toluene}/ml_{adsorption\ bed}$. Thus, in terms of monolithic samples the reduction in the channel width was the most important factor in improving their dynamic adsorption capacities, leading to a more than fourfold increase, while reduction in the wall thickness did not cause any improvement.

For the solid extrudates the breakthrough time was reached after 16.3 h while for the tubes breakthrough was at 34.7 h which corresponded to normalised adsorptions of 0.065 and 0.139 $ml_{toluene}/ml_{adsorption\ bed}$. Thus, the hollow tube, with the same external diameter but much greater geometric surface area more than doubled the adsorption capacity of the solid extrudate. This was probably due to the turbulent flow in the adsorption beds when the extrudates and tubes were used leading to a much better contact of the gas to be treated and the walls of the ceramic composite.

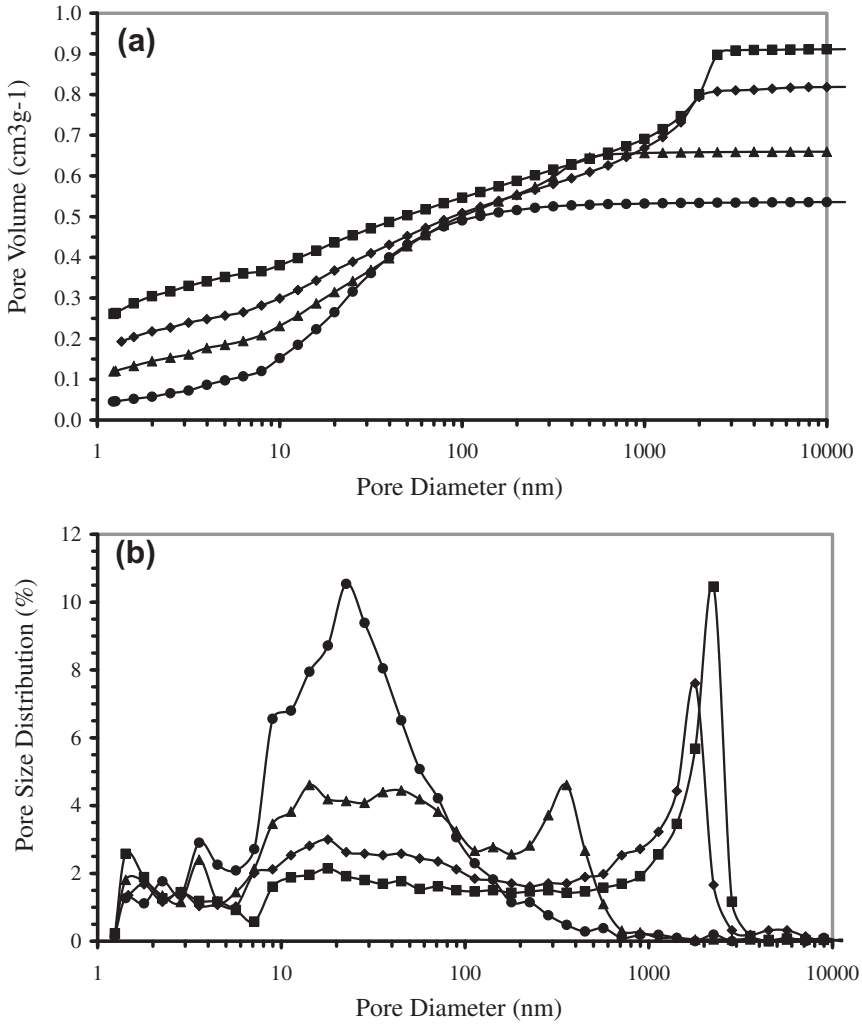

Fig. 3. (a) Total cumulative pore volumes for conformed materials heat-treated at 500 °C Pansil 100/AC: 100/0 ●, 75/25 ▲, 50/50 ♦, 25/75 ■. (b) Pore size distribution curves for conformed materials heat-treated at 500 °C Pansil 100/AC: 100/0 ●, 75/25 ▲, 50/50 ♦, 25/75 ■.

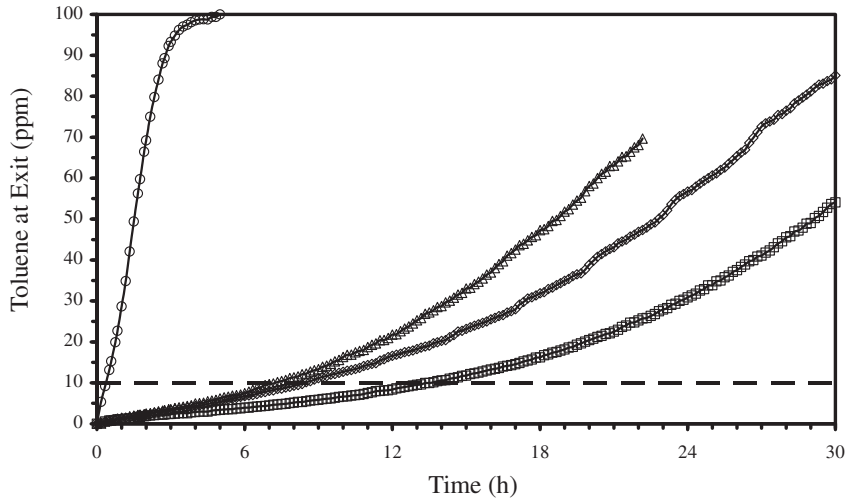

Fig. 4. Breakthrough curves for the dynamic adsorption of toluene at 30 °C for wide channel/thick wall monoliths heat-treated at 500 °C Pansil 100/AC: 100/0 ○, 75/25 △, 50/50 ◇, 25/75 □.

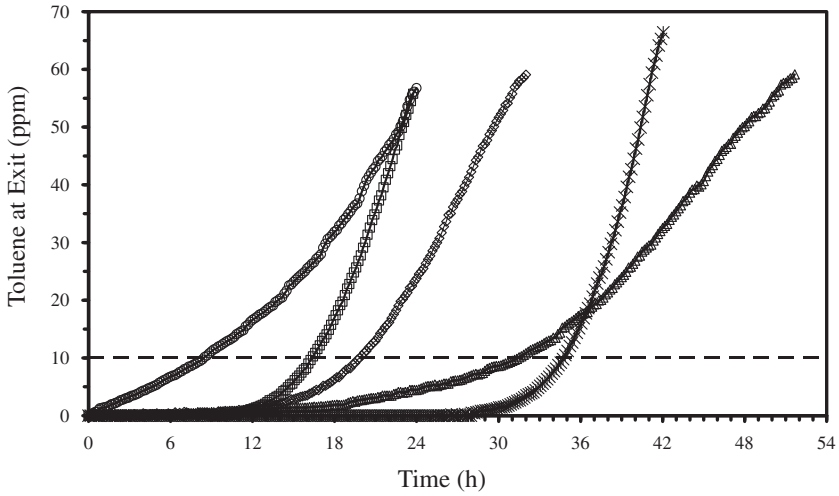

Fig. 5. Breakthrough curves the dynamic adsorption of toluene at 30 °C on Pansil 100/Fluesorb B 50/50 conformed materials heat-treated at 500 °C of various geometries: wide channel/thick wall monolith ○, narrow channel/thick wall monolith △, narrow channel/thin wall monolith ◇, cylinder □ and tube ⁎.

4. Conclusions

In this study the dynamic adsorption capacity for a series of ceramic composites towards toluene at 30 °C was determined. The results showed that under sever conditions of a 0.25 s contact time the most important feature in limiting the dynamic adsorption capacity of open channel monolithic adsorption beds was the width of the open channel. Reduction in the channel width from 2.5 to 2.0 mm led to a fourfold increase in the amount adsorbed. However, reduction in the wall thickness had a negligible effect on the amount adsorbed, indicating that the largest difficulty towards achieving high adsorption capacities under dynamic conditions was the diffusion of the gas to be treated into the composite. For solid extrudates and hollow tubes of the same external diameter the greater geometric area of the latter led to a doubling of the adsorption capacity.

Acknowledgements

This work has been supported by the CICYT project MAT2009-09960, Community of Madrid project S-0505/MAT/000227 and CDTI IDI-20091139.

References

[1] M. Iley, H. Marsh, F. Rodriguez-Reinoso, Carbon 11 (1973) 633.
[2] M. Domingo-Garcia, I. Fernandez-Morales, F.J. López-Garzón, C. Moreno-Castilla, Langmuir 7 (1991) 339.
[3] F.J. López-Garzón, I. Fernández-Morales, C. Moreno-Castilla, M. Domingo-García, in: A. Dabrowski (Ed.), Adsorption and its Applications in Industry and Environmental Protection, vol. 120, Elsevier, Amsterdam, 1998, p. 397.
[4] S.J. Gregg, K.S.W. Sing, Adsorption Surface Area and Porosity, Academic Press, London, 1982.
[5] S.S. Barton, M.J.B. Evans, J. Holland, J.E. Koresh, Carbon 22 (3) (1984) 265.
[6] E.N. Ruddy, L.A. Carroll, Chem. Eng. Prog. (July) (1993) 28.
[7] R.K. Shah, A.L. London, Dept. Mech. Eng., Stanford University, CA, Tech. Rep. 75, 1971.
[8] M. Yates, J. Blanco, P. Avila, M.P. Martin, Micropor. Mesopor. Mater. 37 (2000) 201.
[9] M. Yates, J.A. Martin, M.A. Martín-Luengo, J. Blanco, Micropor. Mesopor. Mater. 65 (2003) 219.
[10] M. Yates, J. Blanco, M.A. Martín-Luengo, Stud. Surf. Sci. Catal. 144 (2002) 569.
[11] S. Brunauer, P.H. Emmett, E. Teller, J. Am. Chem. Soc. 60 (1938) 309.
[12] J. Rouquerol, D. Avnir, C.W. Fairbridge, D.H. Everett, J.H. Haynes, N. Pericone, J.D.F. Ramsay, K.S.W. Sing, K.K. Unger, Pure Appl. Chem. 66 (8) (1994) 1739.
[13] B.C. Lippens, J.H. de Boer, J. Catal. 4 (1965) 319.
[14] B.C. Lippens, B.G. Linsen, J.H. de Boer, J. Catal. 3 (1964) 32.
[15] E.W. Washburn, Proc. Natl. Acad. Sci. USA 7 (1921) 115.
[16] F. Rouquerol, J. Rouquerol, K. Sing, Adsorption by Powders and Porous Solids, Academic Press, London, 1999.
[17] M. Yates, Part. Part. Syst. Char. 23 (2006) 94.